Assessment of Hashin's failure Criteria in Finite Element Modelling of Orthogonal Cutting of Fiber-reinforced Composites

Mohammadreza Moeini[1*], Sardar Malek[2], Keivan Ahmadi[1],

[1]Department of Mechanical Engineering, University of Victoria, Victoria, Canada
[2]Department of Civil Engineering, University of Victoria, Victoria, Canada
[*]Corresponding author. Email: mmoeini@uvic.ca

Abstract—Fiber-reinforced composite materials are widely used in aerospace structures because of their high stiffness, high strength and high fatigue properties. Yet, machining of this type of materials during manufacturing is still challenging because of the undesirable and unwanted damage around the machining area. To avoid that, finite element simulation paves the way to predict the induced damage and to customize the machining parameters. How to develop a robust finite element model for composite machining, however, is still an open question due to the complexity of the failure mechanisms of fiber-reinforced composite. Although in the previous research the simulations were experimentally validated, our literature review shows that there is still a research gap at the level of verification and convergence of the results. In this study, we built a 2D finite element model to predict the reaction force over the cutting tool during orthogonal cutting of glass fiber-reinforced composites. Verification was conducted in the context of mesh refinement and convergence study. Two finite element problems were solved; one material without any failure criteria and one with Hashin failure criteria were examined. The results show that the former converged for the element size of less than 0.008 mm and the later did not converge even at a very fine mesh with an element size of 0.004 mm. Adding a damage model to the contact simulation of orthogonal cutting of composite materials significantly amplified the discretization error. The predicted maximum cutting force decreased 97% when the element size was decreased from 0.01 mm to 0.004 mm. Hence, we believe more comprehensive research is needed on verification of existing material models for simulation of machining of composite.

Keywords-component—**Orthogonal Cutting, Finite Element Method, Composite, Failure Criteria, Convergence Study**

I. INTRODUCTION

Fiber-reinforced plastics (FRP) have been widely used for advanced structures because of their light weight and high strength. Machining process such as trimming and drilling is a very common way to shape fiber-reinforced composite structures during manufacturing. Yet, the machining of such materials is very difficult due to the anisotropic and heterogeneous microstructures. Providing a finishing surface with high quality has been found extremely difficult [1]. During machining, different failure mechanisms of the material can happen [2]. Literature reports serious defects including delamination, burrs, tearing and surface cavities [2, 3]. Moreover, the contacting of the cutting tool edge and the reinforced composite generates a thermomechanical loading which may cause glass transition failure in matrix [3]. The induced defects not only affects the surface finishing but also reduces the loading capacity and the fatigue strength of the machined parts [4, 5]. The strength reduction might lead to a catastrophic fracture when the machined part is subjected to a cyclic and dynamic loading such as in aerospace applications. This motivates researchers to conduct Finite Element (FE) simulations to predict the mechanical behaviour of FRP during machining process [3, 6] and orthogonal cutting [7].

There are three main groups of FE simulation of orthogonal cutting in the literature; explicit modelling, multiscale (homogenization) modelling and a combination of both of them [8]. In the explicit modelling the composite components, including fiber, matrix, and their interface are explicitly meshed and for each of them a failure criteria and damage evolution are defined. In the homogenized modelling, the effective properties of the composite are injected into a continuous domain and composite failure criteria such as Hashin criteria are employed to model the damage. In the third group, authors explicitly mesh the components (*i.e.*, fiber, matrix and the interface) near to the cutting point, but they used the homogenized model far from the cutting point. In all cases, the quality of

mesh extremely affects the predictions of the simulation. The contact simulation, the defined damage initiation criteria and damage evolution makes the convergence a very difficult procedure. In the explicit modelling, for instance, the convergence of the solution is very sensitive to the size of the cohesive element at the interface [9]. In the homogenized modelling, the predicted cutting force reduces almost 90% when the number of elements were increased from 180 to 360 in a 2D plane-stress problem using Tsai-Hill failure criterion [10].

Our literature review, however, indicated that a systematic time-step or mesh convergence study of the FE simulations is usually not included in the reported works. Table I shows a list of the previous FE simulations in the levels of verification and validation. To the best of our knowledge, previous papers only reported the experimental validation in which mostly the predicted cutting force (F_c parallel to the direction of cutting) and/or the thrust force (F_t perpendicular to the direction of cutting) were compared to the experimental measurement.

The objective of this paper is to assess the performance of Hashin failure criteria within a mesh refinement convergence study to predict the cutting force. Section II presents a background of the selected experimental setup from the literature as well as our method to build the FE model. Section III presents the results and finally section II concludes the paper.

II. Background and Methods

The finite element simulation was developed using `Abaqus` (version 2019) and according to the experimental and numerical research of [13] and [15]. The same assumption of [1] was assumed in this modelling:

- The plastic, viscoelastic and thermal deformations of the material were neglected.
- The heat flux generated on the cutting tool and on the work-piece was neglected.
- The deformation of the cutting tool was neglected and thus it was modeled as a rigid body.

TABLE. I: FE simulations of orthogonal cutting

Authors	Ref.	Year	Valid.	Conv.
Arola et al.	[1]	1997	✓	–
Ramesh et al.	[11]	1998	–	–
Mahdi et al.	[10]	2001	✓	–*
Arola et al.	[12]	2002	✓	–
Bhatnagar et al.	[13]	2004	✓	–
Nayak et al.	[14]	2005	✓	–
Rao et al.	[9]	2007	✓	–
Lasri et al.	[15]	2009	✓	–
Aliaji et al.	[16]	2015	✓	–
Abena et al.	[17]	2017	✓	–
Yan et al.	[18]	2019	✓	–
Fu et al.	[19]	2022	✓	–
Zhang et al.	[20]	2022	✓	–
Qin et al.	[21]	2022	✓	–

* The results were reported for two element sizes.

- The effect of the temperature over the mechanical properties of the matrix and fiber was neglected.
- A constant friction coefficient of 0.5 was assumed for the friction contact between the cutting tool and the workpiece [15].
- The process was assumed to be a quasi-static process.
- The FE model consisted of plane-stress elements neglecting the out of plane stress components when compared to those in the cutting plane. Thus, it can be solved through a 2D plane-stress elements rather than 3D solid elements to reduce the computational cost. Note that a plane-strain problem (which is usually used in the cutting of isotropic material) is not valid for FRP due to relatively high out-of-plane displacement [15].

A. Geometry

Figure 1 schematically shows the 2D modelling of orthogonal cutting and Table II indicates the cutting parameters. The workpiece has a dimension of (a_1, a_2, a_3, a_4). The global coordinate is $X - Y$ and the local coordinate (material coordinate) is $1 - 2$. The fiber orientation is θ. The cutting tool has a rake angle of α, a clearance angle of γ and an edge radius of r. The same edge radios of r was considered for the workpiece to remove the sharp edge at the contact point [15].
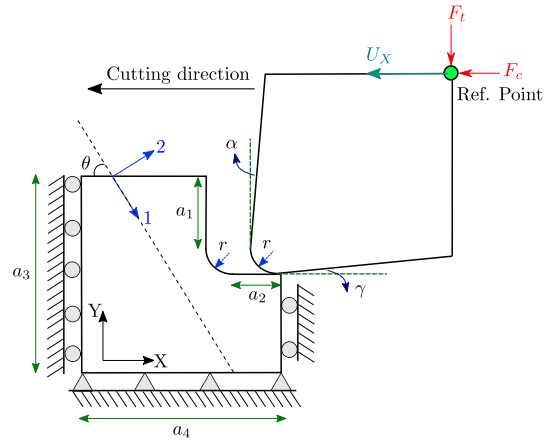

Figure. 1: Schematic representation of orthogonal cutting. The workpiece is a fiber-reinforced composite with a dimension of a_1, a_2, a_3 and a_4 having fiber orientation of θ. The cutting tool is assumed to be a rigid body which is controlled by a reference point. The boundary condition is applied over the reference point. The objective is to compute the reaction force (F_c, F_t) at this point.

B. Boundary conditions

The cutting direction was to the left. The boundary conditions of the left and right sides of the workpiece were $U_X = 0$ and for the bottom side were $U_X = U_Y = 0$, in which U_X and U_Y are the displacement in direction of X and Y. A *Reference Point* was defined at the corner of

the cutting tool and a kinematic constraint in all Degrees of Freedom (DOFs) was set between the Reference Point and the cutting tool. The cutting tool was assumed to be an analytical rigid body. A horizontal displacement was applied over the Reference Point with a value of $U_X = -0.002$ mm, while the other DOFs were fixed. The reaction force, including two components of cutting force (F_c) and thrust force (F_t), was then computed at the reference point.

C. Mechanical properties

The workpiece is a glass fiber-reinforced composite materials with a fiber orientation of $\theta = 0$ whose mechanical properties are indicated in Tables III and IV. The elastic properties extracted from [13]. Bhatnagar et al., however, did not report all the orthotropic properties for the FE simulations. The shear modulus G_{13} and G_{23} also the Poisson ratios ν_{13} and ν_{23} were unavailable and they were assumed to be equal to G_{12} and ν_{12}, respectively.

Hashin failure criteria of `Abaqus` were used to model damage initiation. In Hashin model, the fracture energy of the FRP should be defined for longitudinal and transverse directions as well as for tensile and compressive loading. However, they were not available in [13]. These values for glass fiber-reinforced material were extracted from [22]. It should be noted that in [22] the elastic constants of the material are $E_{11} = 36.9$ GPa, $E_{22} = 10$ GPa, $E_{33} = 10$ GPa, $G_{12} = 3.3$ GPa, $G_{23} = 3.6$ GPa, $\nu_{12} = 0.32$, $\nu_{13} = 0.32$ and $\nu_{23} = 0.44$ which consist of relative difference of 23%, 17%, 17%, 45%, 45%, 40%, 68%, 68%, 132% when compared to the ($E_{11}, E_{22}, E_{33}, G_{12}, G_{23}, G_{13}, \nu_{12}, \nu_{13}, \nu_{23}$) which where we used in the experimental and numerical study of [13] and [15]. For damage evolution, *Linear Softening* was used. Table V shows the damage stabilization parameters (η) in the longitudinal and transverse directions and for the compressive and tensile loading. These constants are used as a viscous regularization scheme to overcome convergence difficulties during the softening behaviour and stiffness degradation [23]. According to `Abaqus` documentation, these constants should be small when compared to the time increment [24]. Large value of η although provides easier time-step convergence, it may violate the physical sense of the simulation. We defined a maximum increment size of 0.1 and a minimum increment size of 1.0×10^{-15} in a general static FE simulation, while the total time was set to 1. In this case, we set η equal to 0.0001.

D. Mesh refinement

Figure 2 shows the mesh of the workpiece. Partitions were used to increase the quality of the mesh and to reduce the number of distorted elements to zero. Two types of elements were used including 8-node rectangular plane-stress element (*i.e.*, `CPS8R`) and 6-node triangular plane-stress element (*i.e.*, `CPS6M`). Note that in these element types each node has 2 DOFs (*i.e.*, U_X and U_Y). In both cases, the element sizes were uniformly refined as $l_{\text{element}} = 0.03, 0.02, 0.01, 0.008, 0.006, 0.005$ and 0.004 mm in the whole domain. The convergence criteria was defined over the maximum predicted cutting force as per:

$$\bar{\Delta} F_{c,\text{max}} = \frac{F_{c,\text{max}}^{\text{fine}} - F_{c,\text{max}}^{\text{coarse}}}{F_{c,\text{max}}^{\text{fine}}} \leq 0.01, \qquad (1)$$

where $\bar{\Delta} F_{c,\text{max}}$ returns the relative difference between the predicted maximum cutting force with a fine mesh ($F_{c,\text{max}}^{\text{fine}}$) against the predicted one by a coarse mesh ($F_{c,\text{max}}^{\text{coarse}}$).

Two FE problems were solved. The first simulation was a simple contact FE simulation on a linearly elastic and orthotropic glass fiber reinforced composite without any failure criteria. The second simulation was a contact FE simulation of the composite featuring damage initiation of Hashin failure criteria. The convergence of these two FE problems was studied to identify the source of the discretization error.

TABLE. III: Mechanical properties of GFRP.

Property	Description	Value
E_{11} [GPa]	Long. modulus [13]	48
E_{22} [GPa]	Trans. modulus [13]	12
E_{33} [GPa]	Out-of-plane modulus	12
G_{12} [GPa]	Shear modulus [13]	6
G_{13} [GPa]	Shear modulus	6
G_{23} [GPa]	Shear modulus	6
ν_{12}	Long. Poisson's ratio [15]	0.19
ν_{13}	Long. Poisson's ratio	0.19
ν_{23}	Trans. Poisson's ratio	0.19
X_t [MPa]	Long. tensile str. [13]	1200
X_c [MPa]	Long. comp. str. [13]	800
Y_t [MPa]	Trans. tensile str. [13]	59
Y_c [MPa]	Trans. comp. str. [13]	128
S_l [MPa]	Long. shear str. [13]	25
S_t [MPa]	Trans. shear str. [13]	250

TABLE. IV: Fracture energy of the composite

Frac. Eng.	Description	Value
G_{XT} [N/mm]	Long. tensile [22]	32
G_{XC} [N/mm]	Long. comp. [22]	20
G_{YT} [N/mm]	Trans. tensile [22]	4.5
G_{YC} [N/mm]	Trans. comp. [22]	4.5

TABLE. II: Orthogonal cutting parameters

Property	Description	Value
α	rake angle [13]	5°
γ	flank angle [13]	6°
r [mm]	tool edge radius [13]	0.05
a_1 [mm]	depth of cut [13]	0.2
a_2 [mm]	left side length	0.1
a_3 [mm]	right side length	0.4
a_4 [mm]	bottom side length	0.4

TABLE. V: Damage stabilization

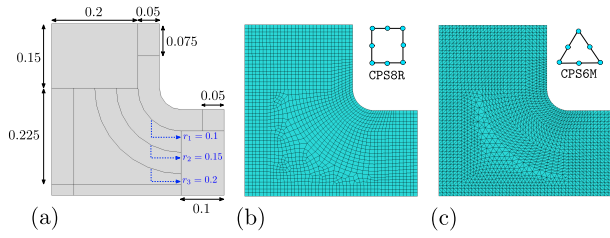| Coefficients	Description	Value
η_{XT}	Long. tensile	0.0001
η_{XC}	Long. comp.	0.0001
η_{YT}	Trans. tensile	0.0001
η_{YC}	Trans. comp.	0.0001

Figure. 2: Meshing with element size of 0.008 mm; (a) partitioning the domain to improve the quality of mesh, (b) rectangular element of `CPS8R`, (c) triangular element of `CPS6M`. In both cases, there is no distorted element.

III. Results and Discussions

A. Convergence study

Figure 3 shows the predicted force-displacement curve when there was no failure criteria in the FE simulation. Figure 4 shows the convergence study of this simulation. The result shows that sizes of 0.008 and 0.01 satisfy the convergence criterion using the rectangular and triangular elements, respectively. The discretization error, therefore, is negligible for the contact simulation with linearly elastic material and considering the convergence criteria of Equation 1.
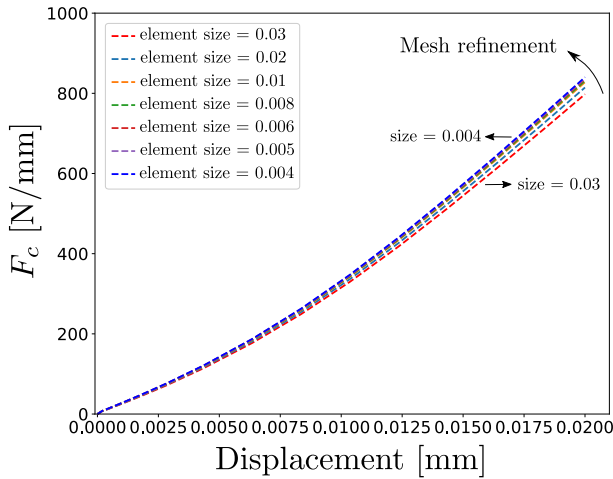
Figure. 3: The predicted cutting force versus horizontal displacement for material with elastic properties and without defining any failure criteria using different element sizes.

Figures 5 and 8 show the predicted force-displacement curve and the convergence study of the orthogonal cutting of composite using Hashin failure criteria. The predicted cutting force suddenly drops when the damage propagation almost reaches the edge. Figure 6 shows the distribution of Hashin failure criteria for the maximum force as well as for the maximum displacement when the element size was 0.008 mm. In this case, Figure 7 shows that the predicted maximum force constantly decreases from 33.0
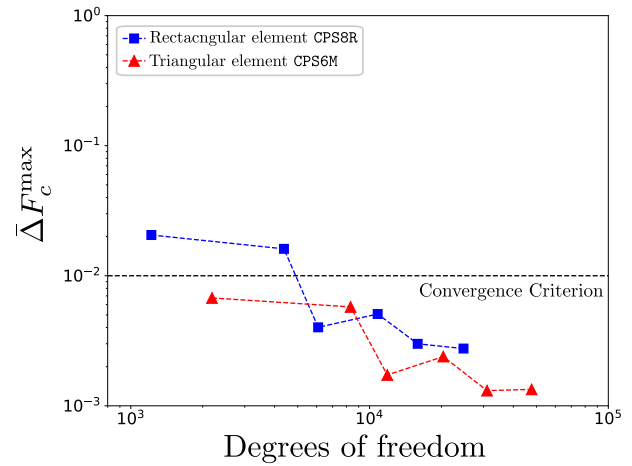

Figure. 4: Mesh size convergence study for modelling the composite without any failure criteria. The predicted maximum cutting force satisfies the given convergence criteria of Equation 1 for the element sizes of 0.008 and 0.01 using rectangular and triangular elements, respectively.

to 16.2 N/mm using rectangular element and it decreases from 40.8 to 16.2 N/mm for the triangular element when the element size decreased from 0.03 mm to 0.004 mm. Consequently, Figure 8 shows that even the element size of 0.004 mm (*i.e.*, 24 744 DOF) could not satisfy the given convergence criterion for both element types. Comparison between Figures 8 and 4, therefore, reveals that the unaccepted discretization error comes from the failure criteria. It should be noted that, in the previous FE simulation, Lasri et al. [15] employed the element size of 0.01 mm using Hashin, Maximum stress, and Hoffman failure criteria. Bhatnagar et al. [13] employed element size of 0.05 mm using Tasi-Hill failure criterion.
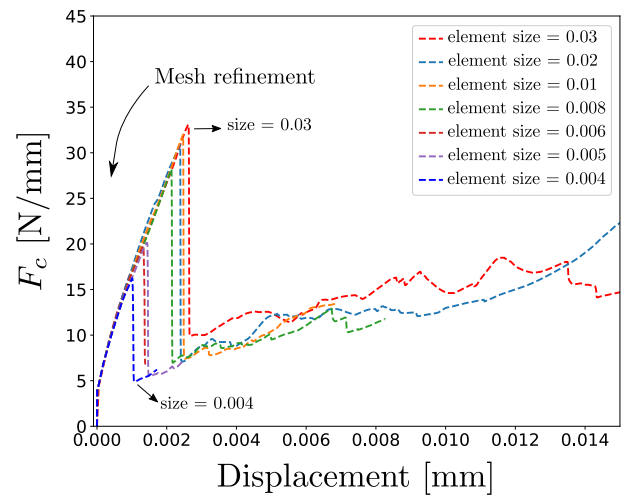

Figure. 5: The predicted cutting force versus horizontal displacement for material with elastic properties with Hishin failure criteria and using different element sizes.
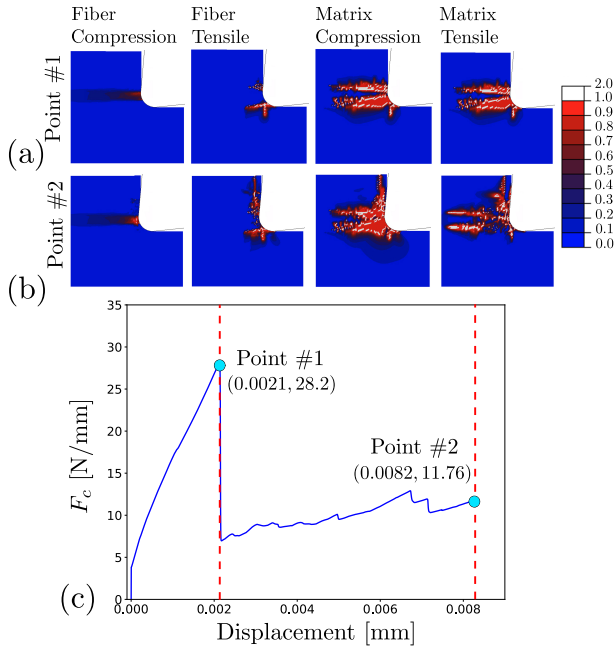
Figure. 6: Distribution of Hashin failure criteria for different modes of damage initiation including fiber compression damage, fiber tensile damage, matrix compression damage and matrix tensile damage at points of; (a) the maximum cutting force, (b) the maximum horizontal displacement, within the (c) predicted force-displacement curve when the element size was 0.008 mm.
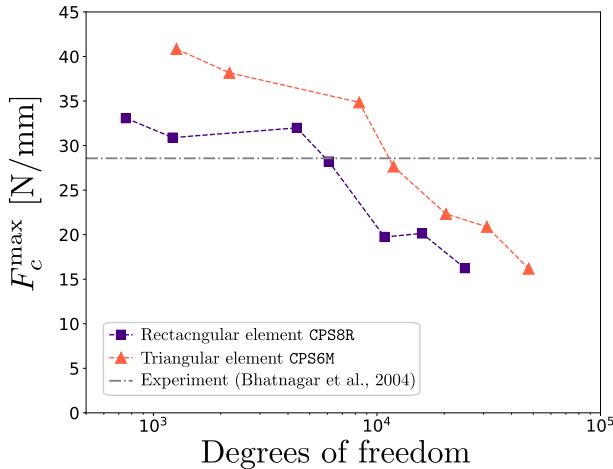

Figure. 7: The predicted maximum cutting force versus the degrees of freedom in the simulation with damage modelling by Hashin failure criteria. The predicted cutting force is constantly decreasing by increasing the degrees of freedom for both rectangular and triangular elements.

IV. Conclusion

This paper highlighted the importance of conducting a proper convergence study as a verification step prior to
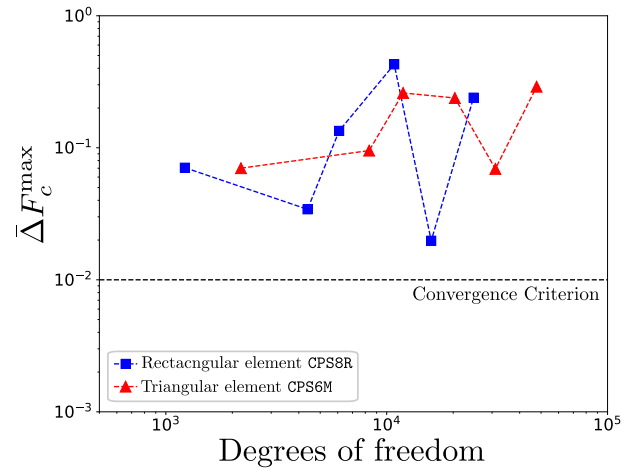

Figure. 8: Mesh size convergence study for modelling the composite with Hashin failure criteria. The predicted maximum cutting force does not converge with respect to the given convergence criteria of Equation 1.

model validation using experimental studies on orthogonal cutting of composites. A simple version of Hashin's failure criteria that has been implemented as a built-in damage model in `Abaqus` was used to highlight the extent of this matter. Our comprehensive mesh refinement convergence study clearly showed that the predicted force was not converged even for a small element size of 0.004 mm due to the nonlinear behaviour of damage initiation and material properties degradation. Hence, we conclude that there is a need to do proper research on the level of verification of the previous failure criteria in the orthogonal cutting of composite structures.

References

[1] D. Arola and M. Ramulu, "Orthogonal cutting of fiber-reinforced composites: A finite element analysis," *International journal of mechanical sciences*, vol. 39, no. 5, pp. 597–613, 1997.

[2] Ş. Yazman, "The effects of back-up on drilling machinability of filament wound gfrp composite pipes: Mechanical characterization and drilling tests," *Journal of Manufacturing Processes*, vol. 68, pp. 1535–1552, 2021.

[3] J. Xu *et al.*, "A critical review addressing drilling-induced damage of cfrp composites," *Composite Structures*, vol. 294, p. 115 594, 2022.

[4] F. Xue, K. Zheng, W. Liao, J. Shu, and D. Miao, "Experimental investigation on fatigue property at room temperature of c/sic composites machined by rotary ultrasonic milling," *Journal of the European Ceramic Society*, vol. 41, no. 6, pp. 3341–3356, 2021.

[5] E. Persson, I. Eriksson, and L. Zackrisson, "Effects of hole machining defects on strength and fatigue life of composite laminates," *Composites Part A: Applied Science and Manufacturing*, vol. 28, no. 2, pp. 141–151, 1997.

[6] N. Shetty, S. Shahabaz, S. Sharma, and S. D. Shetty, "A review on finite element method for machining of composite materials," *Composite Structures*, vol. 176, pp. 790–802, 2017.

[7] L. Han, J. Zhang, Y. Liu, Q. Gu, and Z. Li, "Finite element investigation on pretreatment temperature-dependent orthogonal cutting of unidirectional cfrp," *Composite Structures*, vol. 278, p. 114 678, 2021.

[8] C. R. Dandekar and Y. C. Shin, "Modeling of machining of composite materials: A review," *International Journal of Machine tools and manufacture*, vol. 57, pp. 102–121, 2012.

[9] G. V. G. Rao, P. Mahajan, and N. Bhatnagar, "Micro-mechanical modeling of machining of frp composites–cutting force analysis," *Composites science and technology*, vol. 67, no. 3-4, pp. 579–593, 2007.

[10] M. Mahdi and L. Zhang, "A finite element model for the orthogonal cutting of fiber-reinforced composite materials," *Journal of materials processing technology*, vol. 113, no. 1-3, pp. 373–377, 2001.

[11] M. Ramesh, K. Seetharamu, N. Ganesan, and M. Sivakumar, "Analysis of machining of frps using fem," *International Journal of Machine Tools and Manufacture*, vol. 38, no. 12, pp. 1531–1549, 1998.

[12] D. Arola, M. Sultan, and M. Ramulu, "Finite element modeling of edge trimming fiber reinforced plastics," *J. Manuf. Sci. Eng.*, vol. 124, no. 1, pp. 32–41, 2002.

[13] N. Bhatnagar, D. Nayak, I. Singh, H. Chouhan, and P. Mahajan, "Determination of machining-induced damage characteristics of fiber reinforced plastic composite laminates," *Materials and Manufacturing Processes*, vol. 19, no. 6, pp. 1009–1023, 2004.

[14] D. Nayak, N. Bhatnagar, and P. Mahajan, "Machining studies of ud-frp composites part 2: Finite element analysis," *Machining science and technology*, vol. 9, no. 4, pp. 503–528, 2005.

[15] L. Lasri, M. Nouari, and M. El Mansori, "Modelling of chip separation in machining unidirectional frp composites by stiffness degradation concept," *Composites Science and Technology*, vol. 69, no. 5, pp. 684–692, 2009.

[16] R. El Alaiji, L. Lasri, and A. Bouayad, "3d finite element modeling of chip formation and induced damage in machining fiber reinforced composites," *American Journal of Engineering Research (AJER)*, vol. 4, pp. 123–132, 2015.

[17] A. Abena, S. L. Soo, and K. Essa, "Modelling the orthogonal cutting of ud-cfrp composites: Development of a novel cohesive zone model," *Composite Structures*, vol. 168, pp. 65–83, 2017.

[18] X. Yan, J. Reiner, M. Bacca, Y. Altintas, and R. Vaziri, "A study of energy dissipating mechanisms in orthogonal cutting of ud-cfrp composites," *Composite Structures*, vol. 220, pp. 460–472, 2019.

[19] Q. Fu, S. Wu, C. Li, J. Xu, and D. Wang, "Delamination and chip breaking mechanism of orthogonal cutting cfrp/ti6al4v composite," *Journal of Manufacturing Processes*, vol. 73, pp. 183–196, 2022.

[20] S. Zhang, Y. Li, M. Luo, and C. Shan, "Modelling of nonlinear and dual-modulus characteristics and macro-orthogonal cutting simulation of unidirectional carbon/carbon composites," *Composite Structures*, vol. 280, p. 114 928, 2022.

[21] X. Qin, X. Wu, H. Li, S. Li, S. Zhang, and Y. Jin, "Numerical and experimental investigation of orthogonal cutting of carbon fiber-reinforced polyetheretherketone (cf/peek)," *The International Journal of Advanced Manufacturing Technology*, vol. 119, no. 1-2, pp. 1003–1017, 2022.

[22] S. S. Rahimian Koloor, A. Karimzadeh, N. Yidris, M. Petru, M. R. Ayatollahi, and M. N. Tamin, "An energy-based concept for yielding of multidirectional frp composite structures using a mesoscale lamina damage model," *Polymers*, vol. 12, no. 1, p. 157, 2020.

[23] P. Liu and J. Zheng, "Recent developments on damage modeling and finite element analysis for composite laminates: A review," *Materials & Design*, vol. 31, no. 8, pp. 3825–3834, 2010.

[24] M. Smith, *ABAQUS/Standard User's Manual, Version 6.9*, English. United States: Dassault Systèmes Simulia Corp, 2009.